buildings

MDPI

Article

The Influence of Crystalline Admixtures on the Properties and Microstructure of Mortar Containing By-Products

Jakub Hodul [1,*], Nikol Žižková [1] and Ruben Paul Borg [2]

[1] Faculty of Civil Engineering, Institute of Technology of Building Materials and Components, Brno University of Technology, 602 00 Brno, Czech Republic; zizkova.n@fce.vutbr.cz
[2] Faculty for the Built Environment, University of Malta, 2080 Msida MSD, Malta; ruben.p.borg@um.edu.mt
* Correspondence: hodul.j@fce.vutbr.cz; Tel.: +420-541-147-530

Received: 26 June 2020; Accepted: 18 August 2020; Published: 21 August 2020

Abstract: Crystalline admixtures and industrial by-products can be used in cement-based materials in order to improve their mechanical properties. The research examined long-term curing and the exposure to environmental actions of polymer–cement mortars with crystalline admixture (CA) and different by-products, including Benghisa fly ash and Globigerina limestone waste filler. The by-products were introduced as a percentage replacement of the cement. A crystallization additive was also added to the mixtures in order to monitor the improvement in durability properties. The mechanical properties of the mortar were assessed, with 20% replacement of cement with fly ash resulting in the highest compressive strength after 540 days. The performance was analyzed with respect to various properties including permeable porosity, capillary suction, rapid chloride ion penetration and chloride migration coefficient. It was noted that the addition of fly ash and crystalline admixture significantly reduced the chloride ion penetration into the structure of the polymer cement mortar, resulting in improved durability. A microstructure investigation was conducted on the samples through Scanning Electron Microscopy-Energy Dispersive X-ray Spectroscopy (SEM-EDS). Crystals forming through the crystalline admixture in the porous structure of the material were clearly observed, contributing to the improved properties of the cement-based polymer mortar.

Keywords: polymer–cement mortar; fly ash; crystalline admixture; waste limestone; mechanical properties; microstructure; durability; chloride penetration

1. Introduction

The constituent materials of cement-based materials usually include cement, water, aggregates, admixtures and additives. The binder is a continuous phase in the cement composite and its pore structure is a critical factor, affecting the transport of fluids including gases, liquids and chemical substances in concrete [1]. Materials which are designed to perform in aggressive chemical conditions must be of sufficient durability and should have the capacity to withstand the physical and chemical conditions to which they are exposed, throughout their service life [2]. Cracks have a negative impact on concrete structures, and affect their performance in different ways, including weakening the structure as a result of reduced mechanical properties, or lowering the durability as a result of the penetration of harmful agents into the structure resulting in degradation of reinforcing steel or concrete [3].

Crystalline admixtures can increase the durability of cement-based materials, especially in the case when these materials are exposed to aggressive environments. The catalytic reaction of the chemicals in the crystalline admixture, occurs as long as there is moisture in the cement-based materials. The crystalline admixtures react with calcium hydroxide and other products resulting from the hydration

of the cement [4]. Calcium carbonate is the main healing product which, during 28 days, is able to close cracks up to 400 μm in width [5]. Reiterman et al. [6] confirmed the ability of the repair mortar containing a crystalline admixture to penetrate the concrete surface and form a thin layer with reduced permeability. Crystalline admixtures can positively influence the ability of cement mortars and concrete in reducing the transport of water and chemical aggressive liquids, with improvements in durability [7]. The availability of self-healing technologies, and the control and repair of early-stage cracks in concrete, where possible, could prevent the permeation of fluids, a driving factor for deterioration, thus extending the service life of reinforced concrete structures [8].

Four types of pores occur in cement-based materials. Closed air voids (entrapped air) ranging in size from 1 to several mm and caused by poor compaction have a negative impact on strength. Closed macro-pores with a typical diameter of 10 to hundreds of μm (entrained air) added to accommodate technological needs, decrease the strength of composites as well. Capillary pores form a connected network of mesopores among hydration products, unhydrated cement grains, fines and aggregate, with an average size varying from 10 to 10 μm. These influence mainly durability, because they enable gas and liquid transport by means of diffusion, capillary suction, sorption and ion transport. The finest pores with an average size of 0.5 to 10 nm are called gel pores and are found within the structure of the calcium-silicate-hydrate (C-S-H) phase. These pores are too fine to have any major influence on the strength of the composites, although they directly affect durability and largely shrinkage and creep as well [1,9–12].

Crystalline admixtures (CA) are hydrophilic and they react easily with water, in contrast to water-repellent or hydrophobic products [13]. The crystalline formations produced by CA become a permanent part of the cement matrix [11,14]. The crystallization process, according to the American Concrete Institute (ACI) [14], follows Equation (1), where a crystalline promoter M_xR_x reacts with tricalcium silicates and water, to produce modified calcium silicate hydrates, together with a pore-blocking precipitate $M_xCaR_x - (H_2O)_x$.

$$3CaO - SiO_2 + M_xR_x + H_2O \qquad Ca_xSiO_xR\text{-}(H_2O) + M_xCaR_x\text{-}(H_2O)_x \tag{1}$$

Most supplementary cementitious materials are considered as pollutant by-products, so their reuse would address and partly solve other environmental problems, such as their landfilling. One the most popular additions is fly ash and several researchers [15–17] have noted that cementitious materials, which incorporate the addition of fly ash, have a better performance when compared to materials produced only with Ordinary Portland Cement (OPC). High amounts of fly ash can be used in combination with Portland cement, for the production of concrete covering the range of design strengths which are typically required in practice [18]. Mortars prepared using sustainable cements with fly ash and exposed to Mediterranean climatic conditions, showed adequate service properties in the short term (90 days), similar to or even better than the properties of mortars made with ordinary Portland cement [19,20].

The addition of fly ash has also shown improved performance of cement-based polymer mortars [21]. Waste limestone in concrete, including Globigerina waste limestone, as a partial replacement of Ordinary Portland Cement has been reported to improve the mechanical properties of concrete but also the long-term durability performance determined through water and gas permeability and chloride ion penetration tests [20].

According to the basic requirement No.7 for construction and building materials with CE marking [22], these products have to meet the limits for the appropriate quality of the indoor environment and at the same time minimally burden the external environment. Furthermore, it is necessary to choose suitable energy sources (using renewable energy sources) and also consider the appropriate quality of the product after installation in the building and take into account the economic context necessary for design, operation and disposal (recycling).

The aim of the research presented in this paper was to design mortars using landfilled fly ash, which was produced at the coal-fired power plant in Marsa, Malta, waste Globigerina limestone and

crystalline admixture to improve the properties of mortars. The aim was to investigate the effect of the cement substitution by the fly ash and waste limestone filler, together with the addition of crystalline admixture on the durability of mortars for chloride aggressive environments. The properties were determined after curing at a high relative humidity for 540 days. The mechanical properties of the material were analyzed, together with durability performance through various tests including permeable porosity, capillary suction, rapid chloride ion penetration and chloride migration coefficient.

2. Materials and Methods

2.1. Constituent Materials

2.1.1. Cement

Portland cement CEM I 52.5 N manufactured in Albania, was used as the binder in the research. This cement has the following properties: specific surface area 510 m^2/kg, specific gravity 3410 kg/m^3, initial setting time 150 min and final setting time 190 min.

2.1.2. Dolomite Sand

Dolomite sand delivered from Sicily, Italy, was a major component of the polymer–cement mortar. The dolomite sand with total content of $CaCO_3$ + $MgCO_3$ higher than 95%, was first oven dried and then sieved through a 2.0-mm sieve to achieve the required aggregate portion similar to a standard sand with a granulometry of 0–2 mm. The content of fine particles smaller than 300 μm in the aggregate was 25%.

2.1.3. Waste Limestone

The waste limestone used in the polymer cement mortar is a quarry by-product resulting from the extraction of Globigerina limestone blocks in open pit quarries, from the Lower Globigerina Limestone Member in the Maltese Islands. The waste limestone was sourced from franka type limestone from a quarry in Siġġiewi, Malta. The waste material was dried and then sieved through a 250-μm sieve to remove larger particles and for use as a partial cement replacement material in the mixes.

2.1.4. Fly Ash

The Bengħisa fly ash which was used in the research as the substitute of the cement, was produced at the Marsa Power Station and subsequently landfilled in the Bengħisa quarries, Malta. The fly ash was extracted for the purpose of this research, directly from the quarry where it had been disposed, at a depth of 1 m below the existing soil cover, where the material was observed to be free from soil and any other contaminants. The sample was oven dried for 24 h at 105 °C and sieved on a 125-μm sieve prior to its use as a partial substitute of the cement in the polymer cement mortar. The fly ash thus treated had a specific surface area of 4120 and a specific gravity of 2380 kg·m^{-3}.

2.1.5. Crystalline Admixture

Xypex crystalline admixture produced by Xypex Chemical Corporation was used in the polymer–cement mortar. From a chemical point of view, this admixture is responsible for the generation of a non-soluble crystalline formation, deep within the pores and the capillary tracts of mortars and concrete. It is composed mainly of CaO (45.7%), SiO_2 (11.5%), Al_2O_3 (2.4%) and Fe_2O_3 (1.7%).

2.1.6. Ethylene-Vinyl Acetate Copolymer (EVA)

An Ethylene-vinyl acetate copolymer (EVA) admixture, VINNAPAS 4020N, produced by Wacker Chemie AG was used to improve the properties of fresh and hardened polymer–cement mortars. The fresh mortars benefit through a lower water demand while retaining an extended workability due

to the surface-active compounds in the polymer emulsion. In hardened mortars, EVA copolymer creates a polymer film that improves mechanical properties and absorption properties by sealing pores, preventing the ingress of moisture.

2.1.7. Cellulose Ether

A cellulose ether (methylcellulose derivatives) made from cellulose, Culminal manufactured by Ashland was used in the mixes. This type of admixture extends the workability of fresh mortars by increasing its retention capacity and helps improve the properties of the hardened polymer–cement mortar.

2.1.8. Superplasticizer

The main function of the superplasticizers is to reduce the amount of water in the cementitious mixture without reducing workability and consistency. MasterGlenium 51, polycarboxylic ether based, produced by BASF was used in the research.

2.2. Verified Mix Designs

A total of three polymer cement mortar formulations were tested. The individual formulations are distinguished by the type, amount of by-product (fly ash and Globigerina limestone waste) and crystalline admixture. The amount of by-products (fly ash, waste limestone) was chosen on the basis of previous research, when basic properties of the polymer–cement mortars were tested [20]. The amounts of the individual components in the tested mortars, calculated per 1 m^3, as given in Table 1, derived from the bulk density of the mortar in the fresh state, 2200 kg/m^3. To maintain the required consistency (mortar flow table result of 130 mm), it was necessary to add a small amount of water and superplasticizer in the formulation with fly ash, which showed high water absorption during the preparation of the fresh mortar.

Table 1. Composition of the mortars analyzed in [kg/m^3].

Input Materials	REF	WL20-CA	FA20-CA
Cement CEM I 52.5 N	601.5	473.5	473.5
Fly ash	-	-	120.3
Waste Limestone	-	120.3	
Dolomite sand	1310.3	1302.2	1300.3
Ethylene-vinyl acetate copolymer	6.0	6.0	6.0
Cellulose ether	5.0	5.0	5.0
Crystalline admixture	-	8.0	8.0
Superplasticizer	15.3	15.3	15.8
Water	261.9	261.9	271.4
W/C ratio [1]	0.4	0.4	0.4

[1] In the case of FA20-CA and WL20-CA, W/C ratio is the total amount of cement + by-products.

2.3. Test Methodology

2.3.1. Density, Compressive and Flexural Strength

The three-point flexural strength and the compressive strength of the polymer–cement mortars were determined in accordance with EN 196-1 standard. These mechanical parameters were determined after 28, 60, 90, 180 and 540 days of curing in an environment with high relative humidity (90%) and a temperature of 20 °C, using a climatic chamber. Three samples (40 × 40 × 160 mm) of each mixture of polymer cement mortars were used for flexural strength determination and 6 samples (fragments of beams after flexural strength determination) for compressive strength determination. The density of the hardened samples was also determined at different curing times.

2.3.2. Dynamic Modulus of Elasticity

The dynamic modulus of elasticity in compression ($E_{dyn,U}$) was determined with ultrasonic measurement, according to the standard EN 12504-4. Three beams (40 × 40 × 160 mm) of each mixture of polymer cement mortars were used for the determination of $E_{dyn,U}$. The modulus of elasticity was determined after 28, 60, 90,180 and 540 days of curing in an environment with high relative humidity (95%).

2.3.3. Permeable Porosity

The Vacuum Saturation method was used to measure the porosity. The 100-mm-diameter × 50-mm cylinder specimens were used to determine the porosity of the samples and its variation over time for different mixes. The samples were placed in the dessicator under vacuum at a pressure of 90 kPa for 3 h. De-aired water was then drained from a connected second water desiccator to entirely cover the test samples in the first desiccator. The vacuum was maintained for another hour after which air was allowed in slowly and the sample left in the desiccator under water for a further 20 h. The saturated surface dry mass and the buoyant mass of the specimen was determined. The samples were then placed in an oven for a period of not less than 48 h at a temperature of 105 ± 5 °C, such that the oven dry weight did not vary by more than 0.1% between successive readings taken 24 h apart. The vacuum saturation porosity was determined using Equation (2),

$$Permeable\ Porosity\ (\%) = \frac{(Ws - Wd)}{(Ws - Wb)} \quad (2)$$

where *Ws* = Saturated surface-dry mass of the specimen in air (g); *Wd* = Oven-dry mass of the specimen in air (g); *Wb* = water submerged mass of the saturated specimen (g).

2.3.4. Capillary Suction

The capillary suction was conducted with reference to UNE 83982:2008. Before the test, all the lateral surfaces of the samples were sealed with resin. The samples were then dried in an oven at 40 ± 2 °C for 48 h until constant weight was reached. The samples were then placed inside a covered container with water, on specific supports with a water height on the sides of 2 mm.

The amount of absorbed water was obtained as the mass gain at 5, 10, 15 and 30 min and at 1, 2, 3, 4, 5, 6 and 24, 48, 72, 96 h, using a balance with a precision of 0.01 g. Each weighing operation was completed within 30–35 s and the room test temperature was maintained at 20 ± 2 °C throughout the test period.

The absorption curve relating mass gain (Q) and the square root of time ($\sqrt{t}$) was plotted. According to Fagerlund, the curve obtained shows an initial phase ($0 < \sqrt{t} < \sqrt{t_n}$) relating with the water filling due to capillary suction, and a second phase ($\sqrt{t} \geq \sqrt{tn}$) corresponding to the diffusion process of water through the pores. The capillary suction coefficient (K) is calculated using Equation (3),

$$K = 0\frac{\delta_a \cdot \varepsilon_e}{10 \cdot \sqrt{m}} \quad (3)$$

$$\varepsilon_e = \frac{Q_n - Q_0}{A \cdot h \cdot \delta_a} \quad (4)$$

$$m = \frac{t_n}{h^2} \quad (5)$$

where K: capillary suction coefficient ($kg/m^2min^{0.5}$); δ_a: water density (1 g/cm^3); ε_e: effective porosity of concrete (cm^3/cm^3); m: water penetration resistance due to capillary suction (min/cm^2); Q_n: specimen mass once the saturation is reached ($t = t_n$) (g); Q_0: initial specimen mass ($t = 0$) (g); A: specimen section (cm^2); h: specimen thickness (cm); t_n: necessary time to reach the saturation (min).

2.3.5. Chloride Migration Coefficient

The Chloride migration coefficient was determined through NT BUILD 492: "Concrete, Mortar and Cement Based Repair Materials: Chloride Migration Coefficient from Non-Steady State Migration Experiments". The test was carried out on a 100-mm-diameter, 50-mm-thick concrete specimen. The samples were preconditioned and then subjected to 30 V to record the first current value which determined the test voltage and duration.

The non-steady-state migration coefficient D_{nssm} was calculated using Equation (6) in accordance to NT build 492.

$$D_{nssm} = \frac{0.0239 \cdot (273 + T) \cdot L}{(U - 2) \cdot t} \cdot \left(X_d - 0.0238 \cdot \sqrt{\frac{(273 + T) \cdot L \cdot X_d}{U - 2}} \right) \quad (6)$$

where D_{nssm} is the non-steady state chloride migration coefficient (10^{-12} m^2/s); U is the absolute value of the applied potential (V); T is the average value of the initial and final temperatures in the anolyte solution (°C); L is the thickness of the specimen (mm); X_d is the average value of the chloride penetration depth (mm), and t is the test duration (hours).

2.3.6. Rapid Chloride Penetration Test (RCPT)

The rapid chloride penetration test (RCPT) was conducted with reference to the ASTM C 1202 standard. Three specimens, 100 mm in diameter and 50 mm thick were subjected to an applied DC of 60 V for 6 h, exposing one side of the specimen to a sodium chloride solution (3% NaCl by mass) and the other to a sodium hydroxide solution (0.3 N NaOH).

Electric current readings were taken every 30 min over the 6-h test period. The electric current multiplied by time, expressed in coulombs (C), represents the concrete resistance to chloride ion penetration. The standard chloride ion penetrability based on the charge passed is presented in Table 2 (ASTM C1202).

Table 2. Standard chloride ion penetrability based on charge passed.

Charge Passed [C]	Chloride Ion Penetrability (CIP)
>4000	High
2000–4000	Moderate
1000–2000	Low
100–1000	Very Low
<100	Negligible

2.3.7. Helium Pycnometer Absolute Density Test

The absolute density of the specimen was determined using the helium pycnometer. The weight of the samples was determined using digital scales to 4 decimal places and the volume was determined using the helium pycnometer. The sample was placed in the chamber, maintained at a constant temperature and helium was added to the system. The volume was determined a number of times.

2.3.8. Microstructure Analysis (SEM, XRD)

The microstructure analyses of the polymer cement samples were carried out with all tested mixtures WL20-CA, FA20-CA and reference sample for comparison, using the Scanning electron microscope (SEM) TESCAN MIRA3 XMU and X-ray diffraction analysis (XRD). The microstructure analysis was carried out on samples at 540 days, after conditioning in the chamber at a high relative humidity (95%) and at a temperature of 20 °C.

3. Results and Discussion

The mechanical and durability properties based on different test methods, are presented for all test variables considered, including the addition of crystalline admixture and the substitution of cement with waste limestone and fly ash.

3.1. Compressive and Flexural Strength

The flexural strength was determined through the three-point flexural strength test and the results are presented in Figure 1. The compressive strength results are presented in Figure 2. The highest flexural strength and compressive strength of the polymer cement mortar were obtained at 540 days for mortar with 20% replacement of the cement with fly ash. The difference between the initial strength after 28 days and the compressive strength at 540 days was up to 9 MPa. This is the highest increase in strength for all tested mixes. This trend can be attributed mainly to the pozzolanic reaction of the fly ash. The pozzolanic reaction occurs over long-time scales (months to years) as long as calcium hydroxide is present, when there is sufficient water for the reaction to occur and available space for the reaction products. The limestone waste samples also indicated an increase in strength with time. The lowest strengths were recorded for the reference mortar. Based on the achieved results, it can be stated that the addition of waste limestone and Bengħisa fly ash has a positive effect on the mechanical properties of polymer cement mortars. It is reported that the use of crystalline admixtures does not lead to significant improvements in compressive strength [23]. Results obtained indicate that the crystalline admixture slightly increased the compressive and flexural strength, though crystalline admixtures are not intended to increase the compressive strength but rather the durability of cement-based materials [24].

3.2. Dynamic Modulus of Elasticity

The highest values of the dynamic modulus of elasticity were obtained for samples containing waste limestone and crystalline admixture, namely 32.4 GPa after 540 days, as indicated in Figure 3. The highest increase in the modulus of elasticity in the first half year of curing was recorded for the mix with the fly ash content, mainly due to the pozzolanic reaction. In this mix, based on the trend line (Figure 3), there is also a clear logarithmic prediction of the increase in the value of the modulus of elasticity at the time when the highest coefficient of determination was calculated (R^2 = 0.9374). The addition of fly ash can lower the dynamic modulus of elasticity, but this depends also on the fly ash properties (granulometry, chemical composition) and efficiency of pozzolanic reaction. In this case, the polymer cement mortar did not achieve the values of modulus of elasticity of the reference and the WL20-CA mix even after 540 days of aging. Nevertheless, lower value of modulus of elasticity are desirable mainly in the rehabilitation of concrete structures where patch repair mortar is required to have equal or lower values of modulus of elasticity to the original concrete.

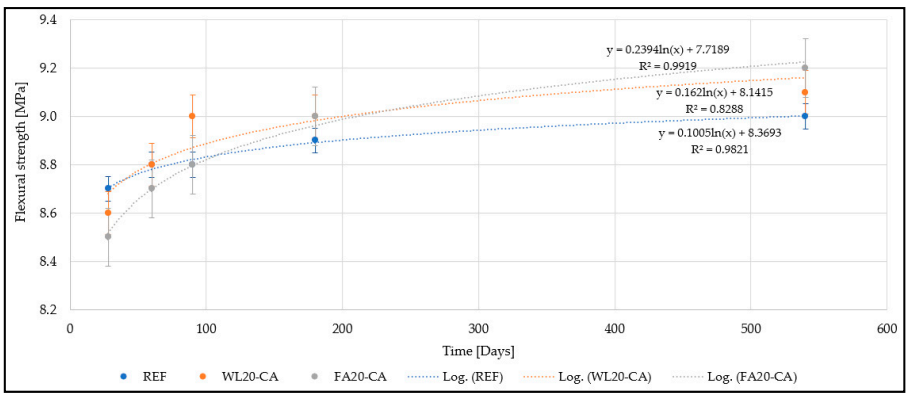

Figure 1. Results of flexural strength including trendlines.

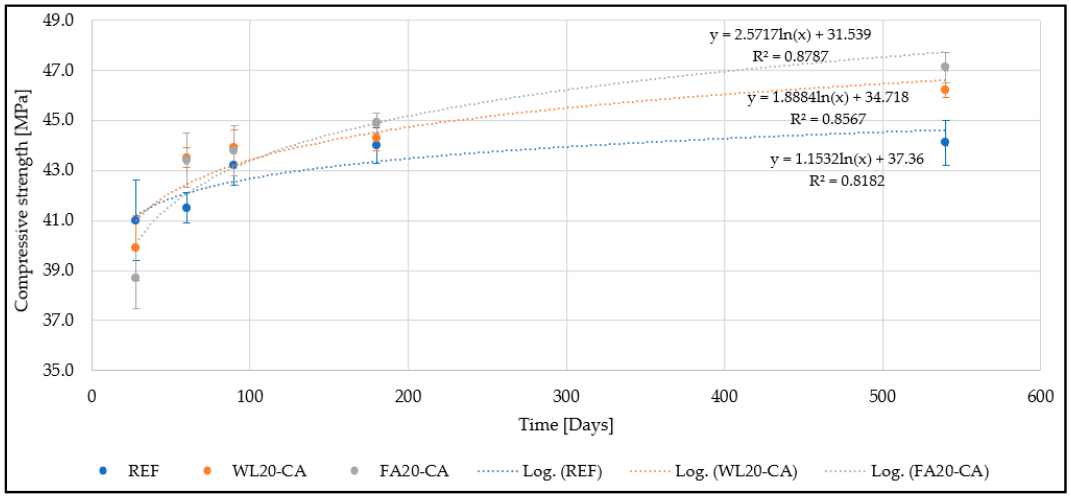

Figure 2. Results of compressive strength including trendlines.

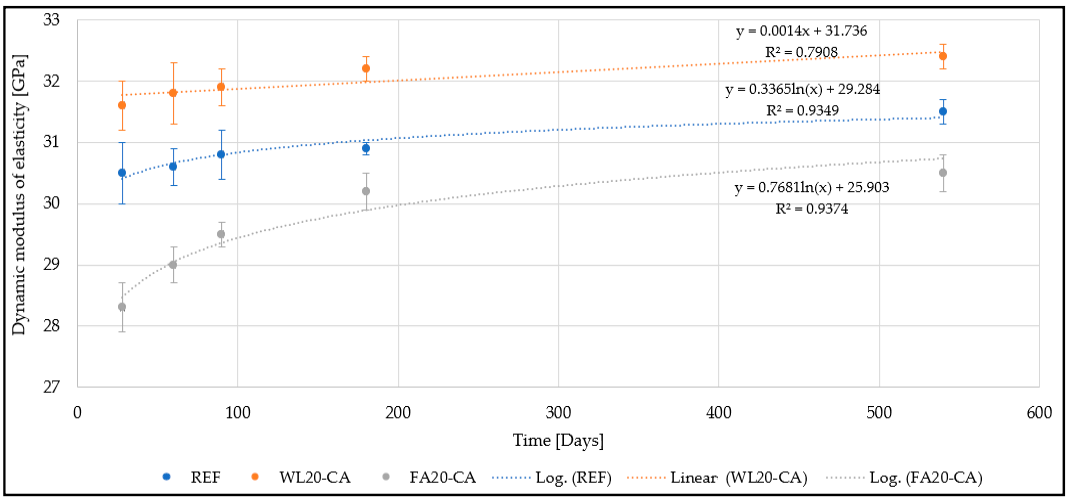

Figure 3. Results of dynamic modulus of elasticity including trendlines.

3.3. Permeable Porosity

The results of permeable porosity, at 540 days are presented in Figure 4. It can be seen that the highest value of permeable porosity was obtained for the reference mix which did not include crystalline admixture nor fly ash or waste limestone. From these results, it is obvious that the crystalline admixture filled the pores of the mortar, reducing the porosity of the samples. The reduction of permeable porosity increases the durability of the polymer–cement mortars and aggressive fluids do not penetrate easily into the inner structure of materials when the permeable porosity is lower. The porosity is observed to also be inversely correlated to compressive strength.

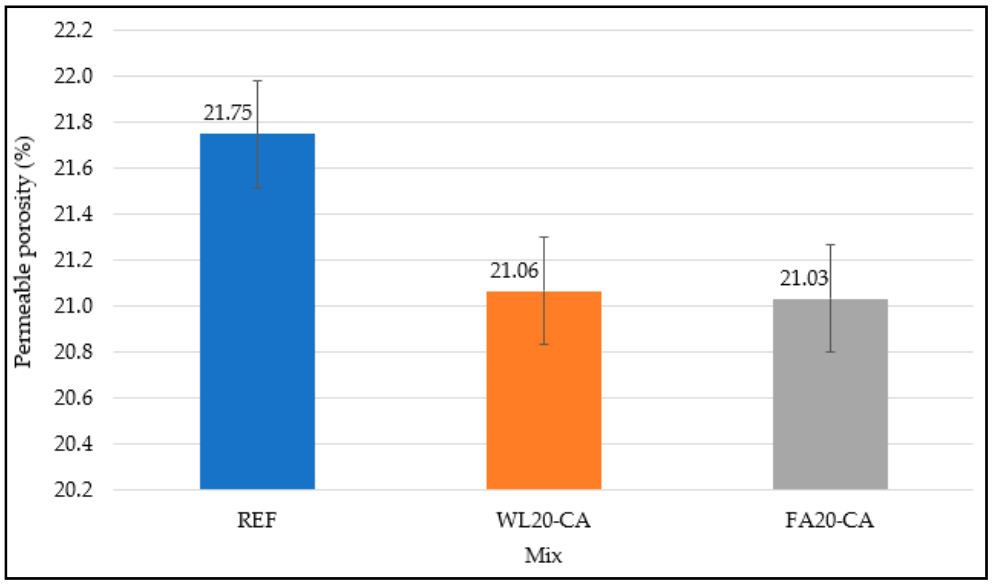

Figure 4. Permeable porosity of polymer–cement mortars.

3.4. Capillary Suction

The water absorption test can be used to assess the healing capability of the polymer–cement mortars containing crystalline admixture [25]. The results of the capillary suction test at 540 days are summarized in Table 3 and the graphical evaluation of the tests is presented in Figure 5. The lowest value of the capillary suction coefficient (K) was achieved with the mix containing fly ash and crystalline admixture indicating an improved durability performance. Generally, the addition of fly ash to polymer–cement mortars and concretes contributes to reduction of the shrinkage and cracking. The low value of capillary sorption obtained for the mortar FA20-CA is indicative of improved performance in the long term.

Table 3. Summary of the capillary suction test results.

Capillary Suction	Unit	REF	WL20-CA	FA20-CA
Effective Porosity (ε_e)	cm^3/cm^3	0.507	0.474	0.300
Capillary Suction Coefficient (K)	$kg/m^2min^{0.5}$	0.000152	0.000144	0.000112

3.5. Chloride Migration Coefficient

The non-steady-state chloride migration coefficients D_{nssm} for different mortars, determned at 540 days with reference to NT Build 492 are presented in Table 4. The highest value of migration coefficient was achieved for the reference mortar. The reference mortar did not contain crystalline admixture and secondary raw materials. The lowest chloride migration coefficient was recorded with the polymer-mortar containing fly ash and crystalline admixture. It is clear from the results that the addition of the crystalline admixture and fly ash had a positive effect in preventing the penetration of chloride ions into the structure of mortars and the addition of these components also increased durability. The pozzolanic reaction of the mortar FA20-CA could have also positive effects on preventing the ingress of chloride ions into the mortar. A high-precision digital caliper was used for the depth readings, shown in Figure 6. It was reported [26] that the addition of fly ash to concrete mixes with granodiorite aggregate, resulted in a reduction of the D_{nssm} value by 38% in comparison with the reference concrete after 28 days of curing, and by 41% after 90 days of curing, respectively. As a result, the level of the resistance to chloride ion penetration increased from unacceptable to acceptable.

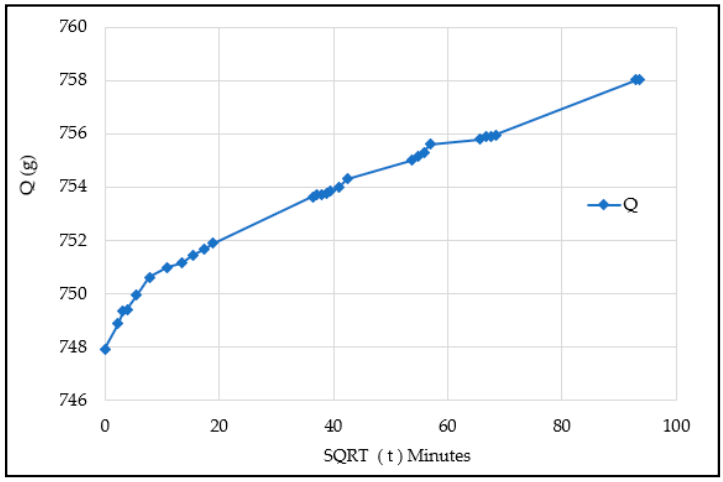

(**a**)

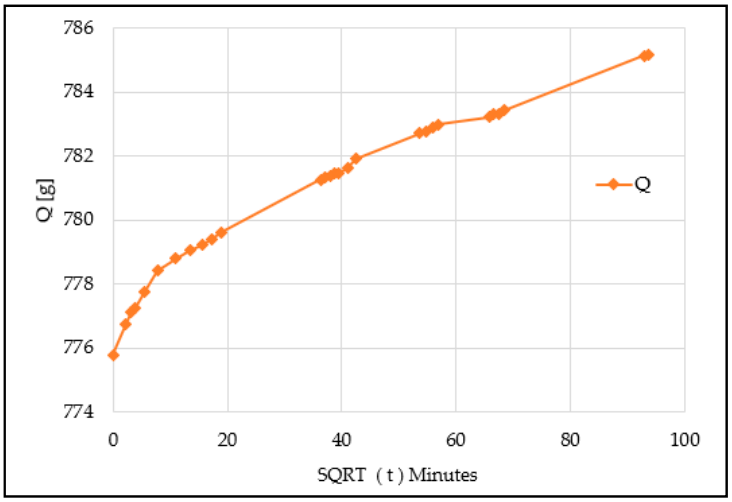

(**b**)

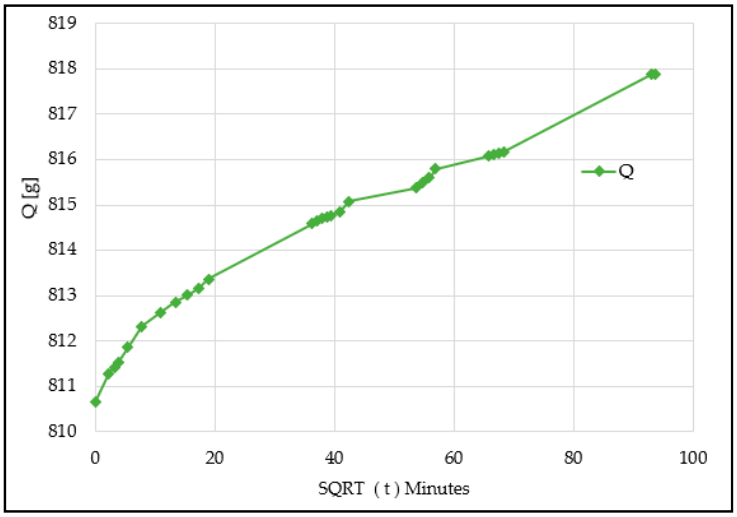

(**c**)

Figure 5. Graphical evaluation of the capillary suction test: (**a**) REF mortar; (**b**) WL20-CA mortar; (**c**) FA20-CA mortar.

(**a**) (**b**) (**c**)

Figure 6. Mortar specimen (100 × 50 mm thick) on completion of the chloride migration coefficient test, split and sprayed with $AgNO_3$ solution. Measurement of chloride penetration depths: (**a**) REF; (**b**) WL20-CA; (**c**) FA20-CA.

Table 4. The chloride migration coefficient test results.

Chloride Migration Coefficient	REF	WL20-CA	FA20-CA
$D_{nssm} \times 10^{-12}$ (m^2/s)	8.45	6.68	1.53

3.6. Rapid Chloride Penetration Test (RCPT)

The rapid chloride penetration test results at 540 days are presented in Table 5 for the Reference mortar (REF) and for the mortars with industrial by-products and crystalline admixtures; mixes WL20-CA and FA20-CA. The reference sample and the polymer–cement mortar with waste limestone and crystalline admixture demonstrated a moderate permeability. The polymer–cement mortar containing fly ash and crystalline admixture exhibited very low chloride permeability. Based on the results (Table 5), it was again confirmed that mortars with fly ash and a crystalline admixture show a lower permeability to chloride ions. Samples were tested after 540 days curing, and therefore this fact can be attributed to both the formation of crystal neoplasms in the pores and the pozzolanic reaction. It can be seen from the RCPT test results that the combination of the fly ash and crystalline admixture can show a very positive effect on the durability of polymer cement mortars. The change of current and temperature during the tests is presented in Figures 7 and 8, respectively. An increase in temperature is indicative also of a higher chloride penetration.

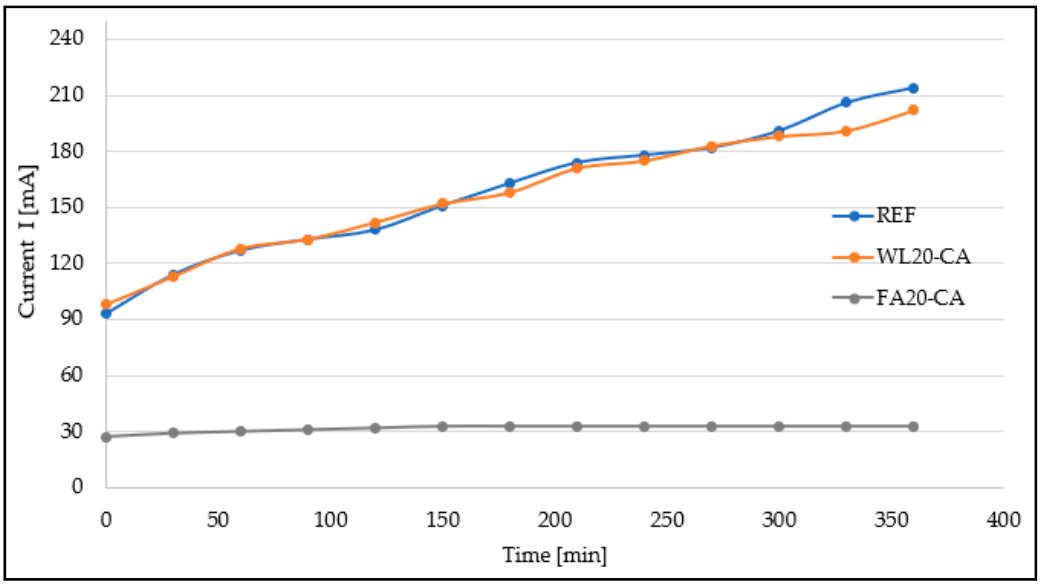

Figure 7. Graphical representation of the variation of current with time.

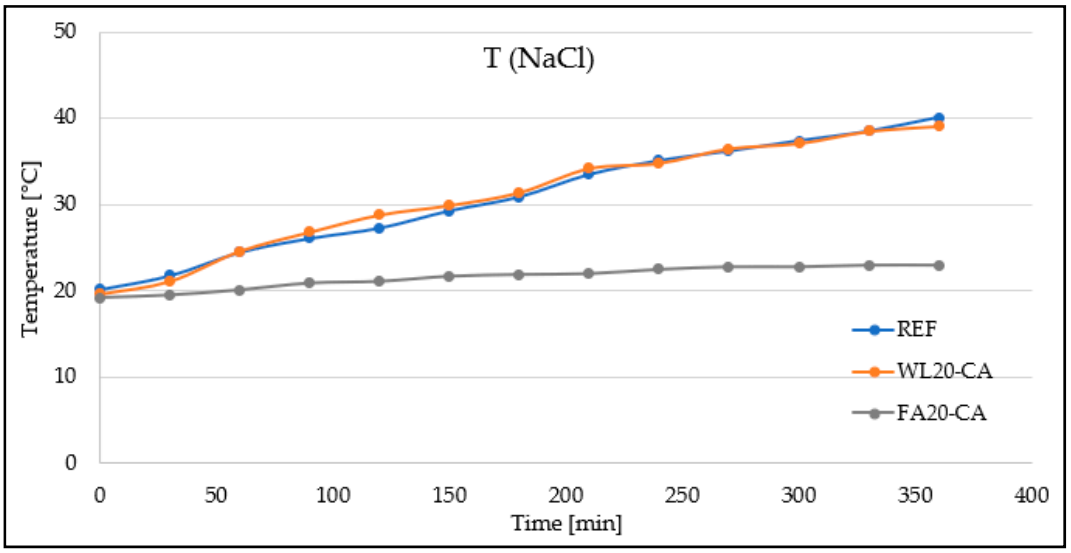

Figure 8. Graphical representation of the variation of temperature with time.

Table 5. Rapid chloride penetration charge passed (ASTM C1202).

Mixture	Q_s [C]	CIP
REF	3115	Moderate
WL20-CA	3072	Moderate
FA20-CA	625	Very Low

3.7. Helium Pycnometer Absolute Density Test

The absolute density was determined using the Helium Pycnometer for the measurement of the volume. The highest density was obtained for the reference mortar whereas the lowest density (2.458 g/cm^3) was obtained with the polymer–cement mortar containing waste limestone and crystalline admixture (WL20-CA). This is probably due to lower density of the waste limestone. However, the differences in the absolute density are not so significant, as can be seen in Table 6. The results are based on an average of three tests for each polymer–cement mortar.

Table 6. Helium pycnometer absolute density test results.

Sample	Pore Volume (V_p) (cm^3)	Standard Deviation σ V_p (cm^3)	Absolute Density (ρ_{ab}) (g/cm^3)	Standard Deviation σ ρ_{ab} (g/cm^3)
REF	0.204	0.001	2.503	0.008
WL20-CA	0.335	0.002	2.458	0.012
FA20-CA	0.313	0.001	2.472	0.009

3.8. Microstructure Analysis (SEM, XRD)

3.8.1. Scanning Electron Microscopy (SEM)

SEM analysis was conducted on the waste globigerina limestone, the fly ash and polymer–cement mortars. The Globigerina Limestone waste was analyzed under the scanning electron microscope using a Merlin FE-SEM ZEISS. The SEM micrographs are presented in Figure 9. The morphology of the shells of the fly ash observed by the scanning electron microscope (SEM) using TESCAN MIRA3 XMU is shown in Figure 10. The typical observed shells are globules with a regular spherical shape cenospheres and plerospheres (Figure 10b).

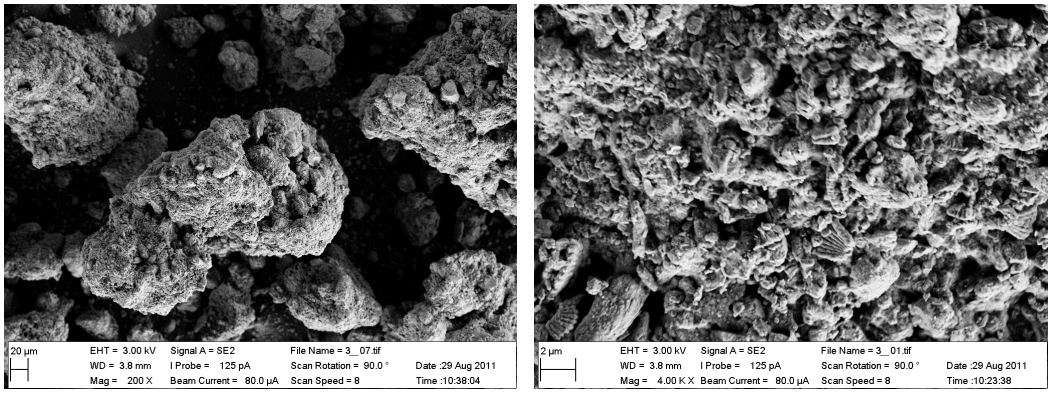

Figure 9. SEM photomicrographs of the Globigerina Limestone waste powder (Siġġiewi, Malta).

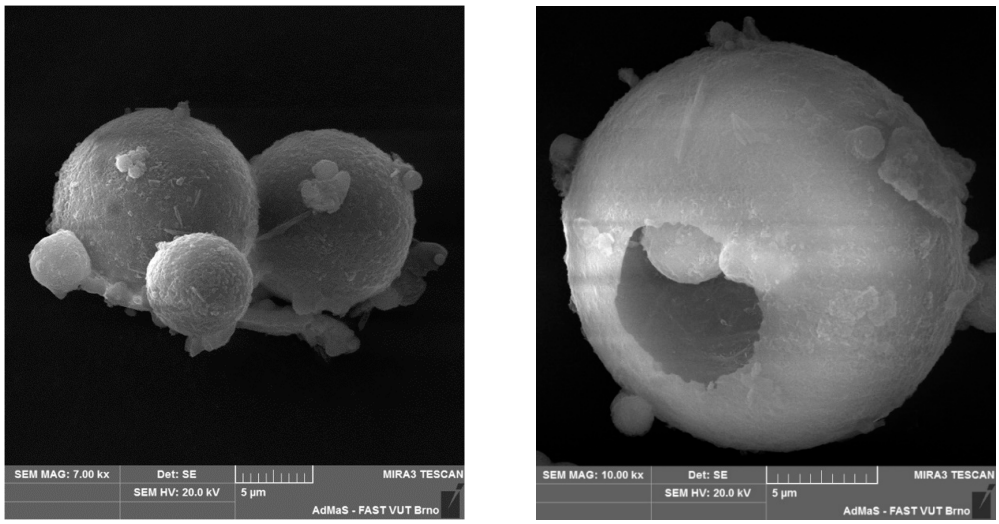

(**a**) (**b**)

Figure 10. SEM photomicrographs of PFA: (**a**) Morphology of the shells of fly ash particles (cenospheres); (**b**) Detail of the shell of fly ash (plerosphere).

The microstructure of the mortars was analysed through SEM. Differences are observed in the microstructure of the reference mortar without CA (Figure 11) and the mortar with CA and fly ash (Figure 12), stored in an environment with high relative humidity, for 540 days. The figures on the right (b) show a magnification of the individual hydration products to better identify their morphology. The mortars containing waste limestone and CA (WL20-CA) clearly show visible newly formed needle-like CA products grouped in "rose" geometries as indicated in Figure 13. The presence of pore-blocking crystals led to a decrease in the total porosity of the matrix (Figure 11). This can also be beneficial in disconnecting the interconnected matrix pore network, resulting in lower permeability values [27]. The chemical reaction between the fly ash particles and portlandite results primarily in the formation of C-S-H gel which could vary in composition and structure [28]. CA in combination with fly ash influences the increase in C-S-H phase content leading to improved strength and durability of the mortar [29].

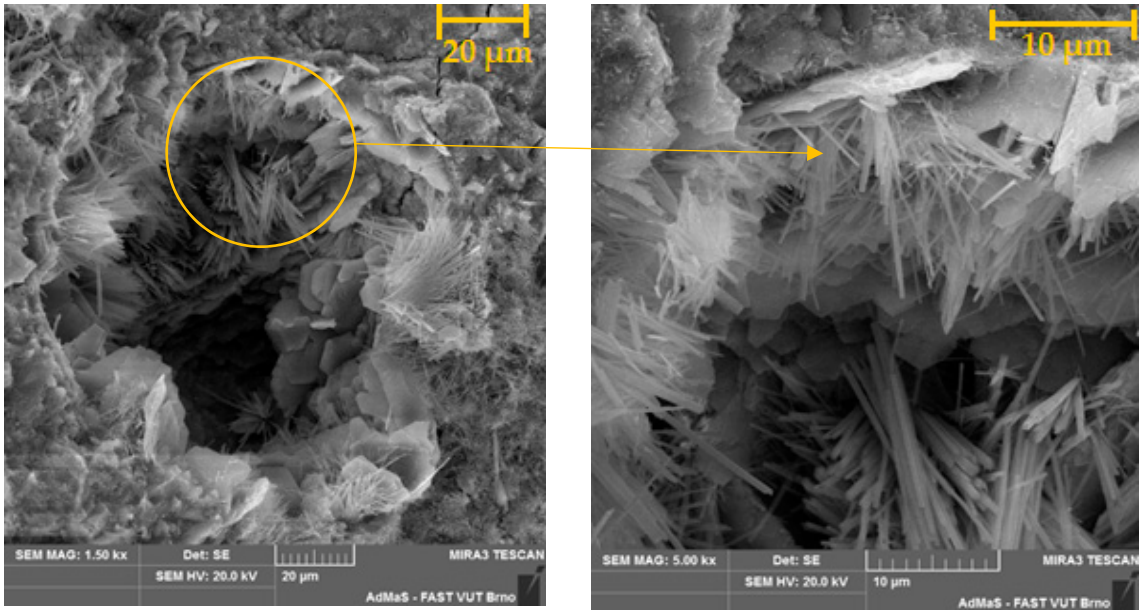

(**a**) (**b**)

Figure 11. SEM photomicrographs of the reference sample REF without CA after 540 days curing at 90% relative humidity: (**a**) Hydration products in the pore of the sample (CSH gels, portlandite, ettringite); (**b**) Detail of ettringite needles and portlandite crystals.

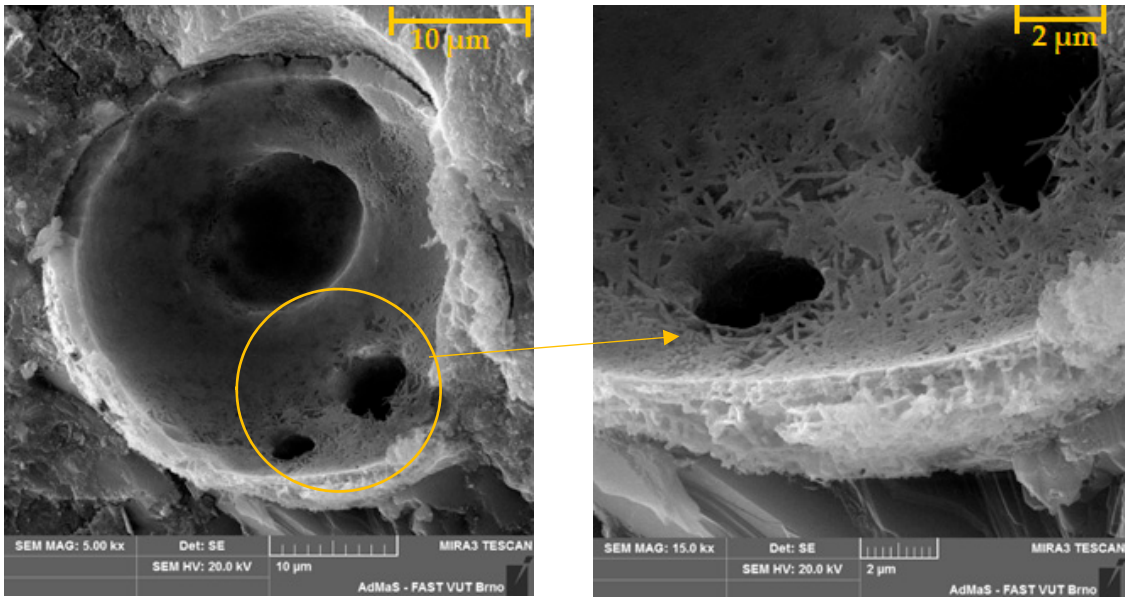

(**a**) (**b**)

Figure 12. SEM photomicrographs of FA20-CA sample after 540 days curing at 90% relative humidity: (**a**) Visible broken cenosphere of thickness 3 µm with micro-holes in the shell; (**b**) Detail of the broken cenosphere with the formation of the C-S-H phase on the surface.

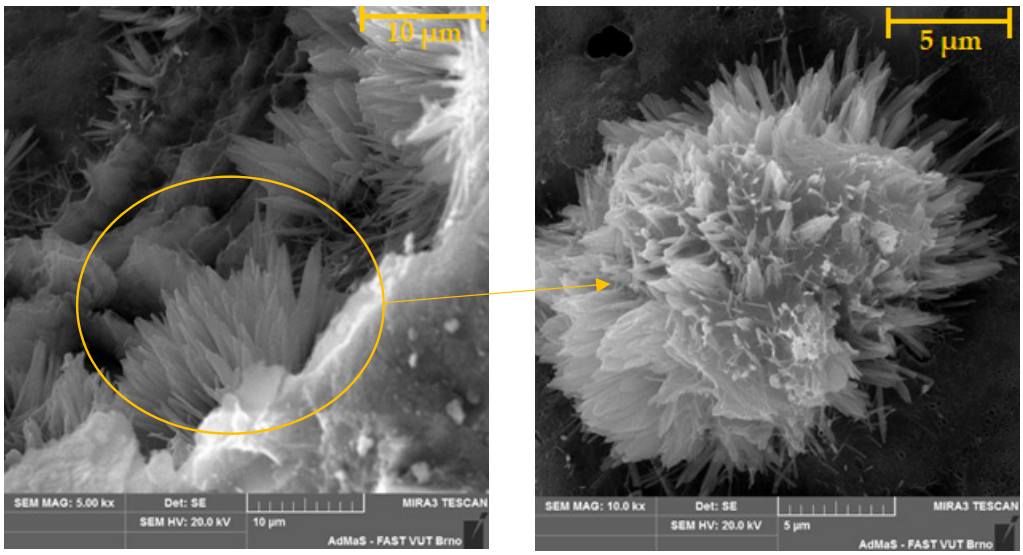

(**a**) (**b**)

Figure 13. SEM photomicrographs of WL20-CA sample after 540 days curing at 90% relative humidity: (**a**) Visible newly formed CA product found in the pore; (**b**) Detail of newly formed CA product found in the pore.

The formation of C-S-H phases can be observed on the surface of fly ash (cenosphere) shells, as seen in Figure 12. It is also obvious from Figure 12a that the thickness of the cenosphere was approximately 3 µm even after 540 days curing in the cement matrix.

3.8.2. X-Ray Diffraction (XRD)

X-ray diffraction analysis was conducted on the waste globigerina limestone, the fly ash and the polymer–cement mortars. The X-Ray diffraction analysis was conducted on the waste limestone powder samples using a Bruker D8 Mo-Source XRD, Bragg-Bentano Optics configuration and is presented in Figure 14. The X-ray diffraction pattern for the Bengħisa fly ash, with mineral peaks for β-quartz, mullite and haematite, can be seen in Figure 15. The distorted baseline is caused because of the high non-crystalline glass content.

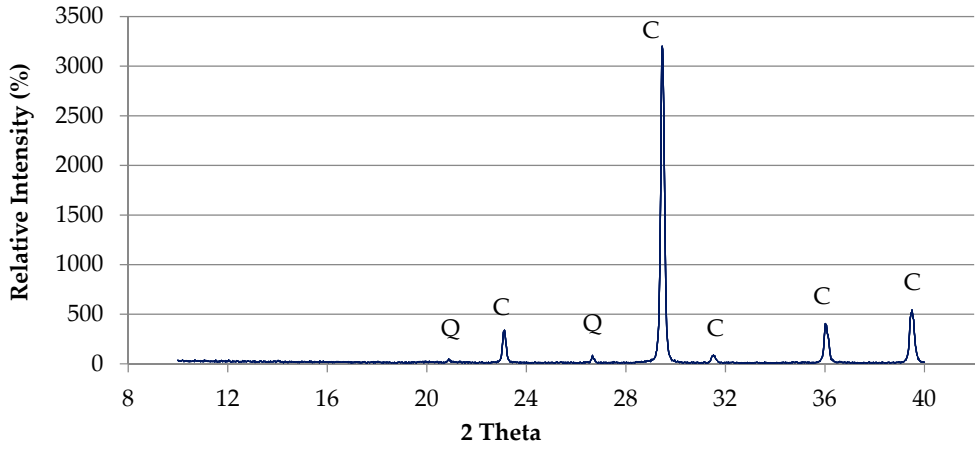

Figure 14. X-ray diffraction pattern of the Globigerina Limestone Filler showing mainly C: Calcite and minor Q: Quartz peaks.

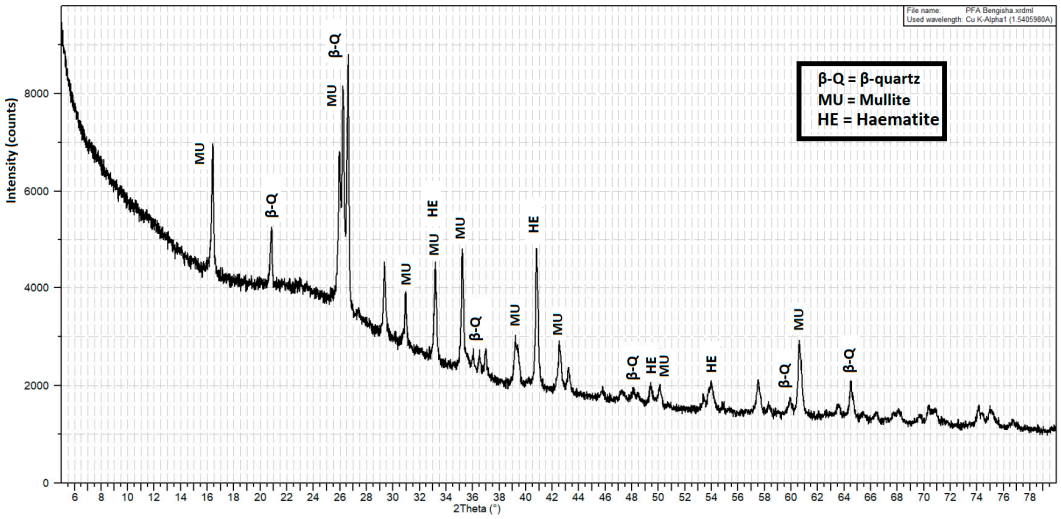

Figure 15. X-ray diffraction pattern of the PFA.

The XRD patterns of the polymer–cement mortars are shown in Figure 16. Based on the XRD analysis, dolomite, calcite, portlandite, ettringite and quartz were identified in all tested mixtures. Samples containing fly ash also contained the same minerals as the reference mortar, with the differences being primarily in the intensity of the individual peaks. Therefore, the labels of the minerals are presented next to the peaks identified on the diffractogram of the reference mortar. The presence of fly ash results in a pozzolanic reaction with the consumption of more $Ca(OH)_2$, as evident in the comparison of the X-ray diffraction pattern peaks for the Reference and WL20-CA mixes, to the FA20-CA mix with fly ash [30].

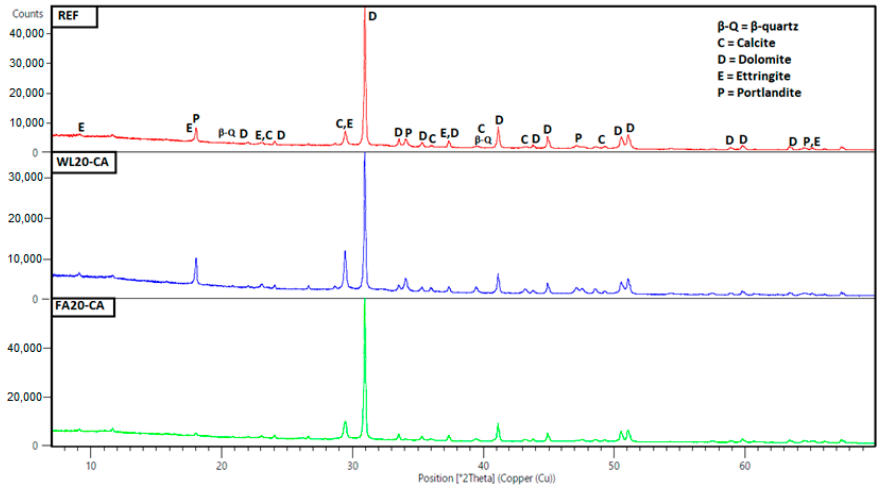

Figure 16. X-ray diffraction pattern of the polymer–cement mortars.

4. Conclusions

In the research presented in this paper, it was concluded that both the mechanical properties and the durability properties of polymer cement mortars are improved by replacing 20% of the cement with the Bengħisa fly ash and by the introduction of crystalline admixture in the mix. Overall, it can be observed that mixes containing secondary raw materials (waste Globigerina limestone, fly ash) showed better performance and have improved properties than the reference mortar, especially in the permeable porosity test, the rapid chloride penetration test, the Chloride migration coefficient test and capillary suction test. This results in a reduction in waste disposal and the potential of recycling of these

waste materials, leading also to a reduction in the consumption of new resources. The best resistance to chloride ion penetration was shown in the case of polymer cement mortar FA20-CA, where fly ash and a crystalline admixture were used. Monitoring of the physical and mechanical properties and durability was supported by an analysis of the microstructure and it was shown that, under suitable conditions (high relative humidity), needle-shaped crystals filling micropores form in the porous structure of the mortar, which prevent the penetration of chloride ions into the internal structure of the mortar. The pozzolanic reaction of the fly ash was also observed, with broken cenospheres and evidence of the formation of C-S-H phases on the surface. Therefore, it has been shown that the use of the fly ash in combination with crystalline admixtures improves the performance of the polymer–cement mortars in coastal areas exposed to chloride ion penetration and the resistance to aggressive environments.

Author Contributions: Conceptualization, J.H. and R.P.B.; methodology, N.Ž. and R.P.B.; formal analysis, R.P.B. and J.H.; investigation, J.H., N.Ž. and R.P.B.; resources, R.P.B.; data curation, J.H. and R.P.B.; writing—original draft preparation, J.H. and R.P.B.; writing—review and editing, J.H. and R.P.B.; supervision, N.Ž.; funding acquisition, J.H. and N.Ž. All authors have read and agreed to the published version of the manuscript.

Funding: This paper was created with the financial support of the Grant Agency of the Czech Republic No. 16-25472S "Dynamics of degradation of cement composites modified by secondary crystallization" and supported by the FAST-S-20-6136 project "Study of the incorporation of hazardous waste and secondary raw materials in a polymer matrix of special composite materials".

Acknowledgments: The research was conducted through collaborative research activity between the Brno University of Technology, Faculty of Civil Engineering and the University of Malta, Faculty for the Built Environment, addressing the use of secondary raw materials in polymer cement mortar and concrete for improved performance.

Conflicts of Interest: The authors declare no conflict of interest.

References

1. Bensted, J.; Rbrough, A.; Page, M.M. Chemical degradation of concrete. In *Durability of Concrete and Cement Composites*; Page, C.L., Page, M.M., Eds.; WoodHead Publishing: Cambridge, UK, 2007; pp. 86–135.
2. Ministerio de Fomento. *EHE-08-Code on Structural Concrete. Articles and Annexes*; Ministerio de Fomento: Madrid, Spain, 2008.
3. Herbert, E.N.; Li, V.C. Self-healing of microcracks in Engineered Cementitious Composites (ECC) under a natural environment. *Materials* **2013**, *6*, 2831–2845. [CrossRef] [PubMed]
4. Rahhal, V.; Bonnavetti, V.; Trusilewicz, L.; Pedrajas, C.; Talero, R. Role of the filler on Portland cement hydration at early ages. *Constr. Build. Mater.* **2011**, *27*, 82–90. [CrossRef]
5. Sisomphon, K.; Copuroglu, O.; Koenders, E.A.B. Self-healing of surface cracks in mortars with expansive additive and crystalline additive. *Cem. Concr. Compos.* **2012**, *34*, 566–574. [CrossRef]
6. Reiterman, P.; Davidová, V.; Pazderka, J.; Kubissa, W. Reduction of concrete surface permeability by using crystalline treatment. *Rev. Română Mater. Rom. J. Mater.* **2020**, *50*, 69–74.
7. Reiterman, P.; Bäumelt, V. Long-term sorption properties of mortars modified by crystallizing admixture. *Adv. Mater. Res.* **2014**, *1054*, 71–74. [CrossRef]
8. Borg, R.P.; Cuenca, E.; Brac, E.M.G.; Ferrara, L. Crack sealing capacity in chloride-rich environments of mortars containing different cement substitutes and crystalline admixtures. *J. Sustain. Cem. Based Mater.* **2017**, *7*, 141–159. [CrossRef]
9. Naik, T.R. *Concrete Durability as Influenced by Density and/or Porosity*; CBU-1997-27; Cement and Concrete Institute of Mexico Symposium "World of Concrete—Mexico": Guadalajara, Mexico, 1997.
10. Zingg, L.; Briffaut, M.; Baroth, J.; Malecot, Y. Influence of cement matrix porosity on the triaxial behaviour of concrete. *Cem. Concr. Res.* **2016**, *80*, 52–59. [CrossRef]
11. Zhao, H.; Xiao, Q.; Huang, D.; Zhang, S. Influence of pore structure on compressive strength of cement mortar. *Sci. World J.* **2014**, *5*, 247058. [CrossRef]
12. Kumar, R.; Bhattacharjee, B. Porosity, pore size distribution and in situ strength of concrete. *Cem. Concr. Res.* **2003**, *33*, 155–164. [CrossRef]

13. Roig-Flores, M.; Pirritano, F.; Serna, P.; Ferrara, L. Effect of crystalline admixtures on the self-healing capability of early-age concrete studied by means of permeability and crack closing tests. *Constr. Build. Mater.* **2016**, *114*, 447–457. [CrossRef]
14. ACI Committee 212. *Report on Chemical Admixtures for Concrete*; Report ACI 212-3R-10; Concrete Institute (ACI): Farmington Hills, MI, USA, 2010; Volume 15, pp. 46–50.
15. Bijen, J. Benefits of slag and fly ash. *Constr. Build. Mater.* **1996**, *10*, 309–314. [CrossRef]
16. Pastor, J.L.; Ortega, J.M.; Flor, M.; López, M.P.; Sánchez, I.; Climent, M.A. Microstructure and durability of fly ash cement grouts for micropiles. *Constr. Build. Mater.* **2016**, *117*, 47–57. [CrossRef]
17. Ortega, J.M.; Esteban, M.D.; Rodríguez, R.R.; Pastor, J.L.; Ibanco, F.J.; Sánchez, I.; Climent, M.A. Long-term behaviour of fly ash and slag cement grouts for micropiles exposed to a sulphate aggressive Medium. *Materials* **2017**, *10*, 598. [CrossRef] [PubMed]
18. McCarthy, M.J.; Dhir, R. Development of high volume fly ash cements for use in concrete construction. *Fuel* **2005**, *84*, 1423–1432. [CrossRef]
19. Ortega, J.M.; Esteban, M.D.; Sánchez, I.; Climent, M.Á. Performance of sustainable fly ash and slag cement mortars exposed to simulated and real in situ Mediterranean conditions along 90 warm season days. *Materials* **2017**, *10*, 1254. [CrossRef] [PubMed]
20. Borg, R.P. Sustainable Concrete: Application of Waste Materials in Concrete and Self Compacting Concrete. Ph.D. Thesis, University of Sheffield, Sheffield, UK, 2014.
21. Žižková, N.; Hodul, J.; Borg, R.P.; Černý, V. Repair mortars containing fly ash and crystalline admixture. *Waste Forum* **2019**, *3*, 254–266.
22. The European Parliament and the Council of the European Union. *Requirements for Construction Products Bearing the CE Marking in Accordance with Regulation (EU)*; No. 305/2011; The Construction Products, Official Journal of the European Union; European Union: Brussels, Belgium, 2011.
23. García-Vera, V.E.; Tenza-Abril, A.J.; Saval, M.; Lanzón, M. Influence of crystalline admixtures on the short-term behaviour of mortars exposed to sulphuric acid. *Materials* **2019**, *12*, 82. [CrossRef] [PubMed]
24. Wang, K.L.; Hu, T.Z.; Xu, S.J. Influence of permeated crystalline waterproof materials on impermeability of concrete. *Adv. Mater. Res.* **2012**, *446–449*, 954–960. [CrossRef]
25. Li, G.; Liu, S.; Niu, M.; Liu, Q.; Yang, X.; Deng, M. Effect of granulated blast furnace slag on the self-healing capability of mortar incorporating crystalline admixture. *Constr. Build. Mater.* **2020**, *239*, 117818. [CrossRef]
26. Glinicki, M.A.; Jóźwiak-Niedźwiedzka, D.; Gibas, K.; Dąbrowski, M. Influence of blended cements with calcareous fly ash on chloride ion migration and carbonation resistance of concrete for durable structures. *Materials* **2016**, *9*, 18. [CrossRef]
27. Azarsa, P.; Gupta, R.; Biparva, A. Inventive microstructural and durability investigation of cementitious composites involving crystalline waterproofing admixtures and portland limestone cement. *Materials* **2020**, *13*, 1425. [CrossRef] [PubMed]
28. Kunther, W.; Lothenbach, B.; Skibsted, J. Influence of the Ca/Si ratio of the C–S–H phase on the interaction with sulfate ions and its impact on the ettringite crystallization pressure. *Cem. Concr. Res.* **2015**, *69*, 37–49. [CrossRef]
29. Reddy, T.C.S.; Ravitheja, A.; Sashidhar, C. Self-healing ability of high-strength fibre-reinforced concrete with fly ash and crystalline admixture. *Civ. Eng. J.* **2018**, *4*, 971–979. [CrossRef]
30. Kwon, Y.H.; Kang, S.H.; Hong, S.G.; Moon, J. Acceleration of intended pozzolanic reaction under initial thermal treatment for developing cementless fly ash based mortar. *Materials* **2017**, *10*, 225. [CrossRef]